

Article

Computational Study of Benzothiazole Derivatives for Conformational, Thermodynamic and Spectroscopic Features and Their Potential to Act as Antibacterials

Adeel Mubarik ^{1,†}, Sajid Mahmood ^{2,†} , Nasir Rasool ^{1,*}, Muhammad Ali Hashmi ³ , Muhammad Ammar ⁴ , Sadaf Mutahir ⁵, Kulsoom Ghulam Ali ¹ , Muhammad Bilal ¹ , Muhammad Nadeem Akhtar ⁶ and Ghulam Abbas Ashraf ^{7,*} 

- ¹ Department of Chemistry, Government College University Faisalabad, Faisalabad 38000, Pakistan; adeelmubarik2@gmail.com (A.M.); kulsoomwajid2011@gmail.com (K.G.A.); muhammadbilalgucuf@gmail.com (M.B.)
- ² Key Laboratory of the Ministry of Education for Advanced Catalysis Materials, Department of Chemistry, Zhejiang Normal University, Jinhua 312004, China; sajidmahmood1987@zjnu.edu.cn
- ³ Department of Chemistry, Division of Science & Technology, University of Education, Lahore 54770, Pakistan; muhammad.hashmi@ue.edu.pk
- ⁴ Department of Chemical Engineering Technology, Government College University Faisalabad, Faisalabad 38000, Pakistan; mammar@gcuf.edu.pk
- ⁵ Department of Chemistry, University of Sialkot, Sialkot 51300, Pakistan; sadafmutahir@hotmail.com
- ⁶ Department of Chemistry, Ghazi University, Dera Ghazi Khan 32200, Pakistan; nakhtar@gudgk.edu.pk
- ⁷ Department of Physics, Zhejiang Normal University, Jinhua 312004, China
- * Correspondence: nasirrasool@gcuf.edu.pk (N.R.); ga_phy@yahoo.com (G.A.A.); Tel.: +92-332-7491790 (N.R.)
- † These authors contributed equally to this work.



Citation: Mubarik, A.; Mahmood, S.; Rasool, N.; Hashmi, M.A.; Ammar, M.; Mutahir, S.; Ali, K.G.; Bilal, M.; Akhtar, M.N.; Ashraf, G.A. Computational Study of Benzothiazole Derivatives for Conformational, Thermodynamic and Spectroscopic Features and Their Potential to Act as Antibacterials. *Crystals* **2022**, *12*, 912. <https://doi.org/10.3390/cryst12070912>

Academic Editors: Younes Hanifehpour, Neil Champness and Patrizia Rossi

Received: 22 April 2022

Accepted: 18 June 2022

Published: 27 June 2022

Publisher's Note: MDPI stays neutral with regard to jurisdictional claims in published maps and institutional affiliations.



Copyright: © 2022 by the authors. Licensee MDPI, Basel, Switzerland. This article is an open access article distributed under the terms and conditions of the Creative Commons Attribution (CC BY) license (<https://creativecommons.org/licenses/by/4.0/>).

Abstract: Benzothiazole analogs are very interesting due to their potential activity against several infections. In this research, five benzothiazole derivatives were studied using density functional theory calculations. The optimized geometry, geometrical parameters and vibrational spectra were analyzed. The charge distribution diagrams, such as FMO (HOMO-LUMO), energies of HOMO-LUMO, polarizability, hyperpolarizability, MESP and density of states, were calculated. The computed energies of HOMO and LUMO showed that the transfer of charge occurred within the compound. The effect of the change of substituents on the ring on the value of the HOMO-LUMO energy gap was also observed. It was observed that, in this series, compound **4** with CF₃ substituent had the lowest energy gap of HOMO-LUMO, and compound **5** with no substituent had highest HOMO-LUMO energy gap. From the energies of HOMO and LUMO, the reactivity descriptors, such as electron affinity (A), ionization potential (I), chemical softness (σ), chemical hardness (η), electronic chemical potential (μ), electrophilicity index (ω), were calculated. In addition, the ¹³C and ¹H NMR chemical shifts of the molecules were calculated using the gauge-independent atomic orbit (GIAO) method; the shifts were in good agreement with the experimental values. The anti-bacterial potential of compounds **1** to **5** was tested by molecular docking studies toward target proteins 2KAU and 7EL1 from *Klebsiella aerogenes* and *Staphylococcus aureus*. Compounds **3** and **1** showed high affinity toward 2KAU and 7EL1, respectively.

Keywords: density functional theory; conformational analysis; benzothiazole; hyperpolarizability; molecular docking

1. Introduction

Benzothiazoles are heterocyclic compounds consisting of two fused rings of benzene and thiazole [1]. Benzothiazole and its derivatives have been very interesting to medicinal and organic chemists as drugs. Benzothiazole is a weak-base heterocyclic compound with a large number of biological activities, such as anti-histamines, anti-virus, schistosomicidal, anti-bacterial, anti-tumor, analgesics, anti-HIV, anti-tuberculosis and anti-inflammatory [2–11]. Malaria is a dangerous and lethal problem due to its higher morbidity

and mortality. *Plasmodium falciparum* is the reason for the occurrence of malaria. Studies have revealed that approximately 212 million people around the world are being infected by malaria in various parts of the world. A dangerous problem is that malaria germs have acquired resistance against different drugs. Benzothiazole derivatives have greater potential biological activity against microbial and malarial infections [12]. 2-aminobenzothiazole is used as a reactant and reaction intermediate, and the endocyclic N-functions and the N-atom are ideally located to enable reactions with bis-electrophilic reagents to synthesize a different variety of heterocyclic compounds [13].

In the last few years, computational chemistry has become an interesting branch for analyzing chemical issues on a laptop or modern computer [14]. It is an associate fast-emerging and exciting discipline that deals with the illustration and also the theoretical calculation of systems, such as drugs, polymers, biomolecules, organic and inorganic complexes and molecules [15]. Our research group already reported the synthesis of benzothiazole derivatives (1–5) and examined their biological activities, such as nitric oxide (NO) scavenging and anti-urease activities [16]. We performed computational studies of the (1 to 5) derivatives to evaluate the thermodynamic and chemical properties by using the DFT approach. Further, a molecular docking analysis was carried out to understand the binding pattern of the studied compounds (1–5) toward target proteins 2KAU and 7EL1 from *Klebsiella aerogenes* and *Staphylococcus aureus*, respectively.

2. Materials and Methods

2.1. Computational Details

Research work was conducted to find the physical characteristics, chemical reactivity and thermodynamic properties of benzothiazole derivatives by using DFT calculations [17]. For the calculation of these properties, three computational software packages were used. All of these calculations were performed on Gaussian 09. In the computations, Becke's three-parameter exchange function was used with the Lee–Yang–Parr non-local parallel-function [B3LYP] with the basis set 6-311G (d,p)/SMD_{1,4-dioxane} level of theory. GaussView was used to visualize the results of quantum mechanical calculations, and GaussSum was used to draw the DOS spectrum. Origin 8.5 was used to draw the UV-Vis and IR spectra. Firstly, the structures of the studied compounds (1 to 5) were optimized. Optimized geometries were used to calculate the thermal and chemical properties. UV-Vis spectra were calculated using the time-dependent density functional theory (TD-DFT) at the same level of theory. Properties such as optimized geometry, frontier molecular orbitals (HOMO-LUMO), energies of HOMO-LUMO, global reactivity parameters, such as electron affinity, ionization energy, chemical softness, hardness, electrophilicity and chemical potential, were calculated [18]. The ¹³C and ¹H nuclear magnetic resonance (NMR) chemical shifts of molecules were calculated using the gauge-independent atomic orbit (GIAO) method; the shifts were in good agreement with experimental values [19]. The structures of benzothiazole's derivatives [16] are given in Figure S1 (see in Supplementary Materials).

2.2. Molecular Docking Analysis

The heteromeric structures of the protein (PDB ID: 7EL1) [20] and urease (PDB ID: 2KAU) [21] were retrieved from the protein database. The proteins were prepared by removing similar binding sites, unnecessary water molecules and refining bond orders. Missing chain atoms were added by using the prime module of Schrödinger suite 2017 [22]. Energy minimization of the proteins was performed using optimized potentials for liquid simulations-3 (OPLS3e) molecular force field with a root-mean-square difference (RMSD) of crystallographic heavy atoms kept at 0.3 Å. Molecular docking of compounds with targeted proteins was performed in Schrodinger 2017.

2.3. Ligand Preparation, Protein Preparation and Grid Generation

All the structures were incorporated into Maestro 11.2 workspace, and then, all the ligands were prepared from the LigPrep menu in their neutral form and organized in a

specific folder. After ligand preparation, protein was downloaded from the RCSB Protein Data Bank (PDB) by using PDB ID (2KAU and 2LE1). Protein was prepared using the Protein Preparation Wizard. The bond orders were assigned, and hydrogen atoms were added. The grid was created by defining the co-crystallized ligand at the active site of the protein. Then, protein was ready for docking and organized in a specific folder.

3. Results and Discussion

3.1. Conformational Analysis

A molecular geometry scan was performed for the identification of possible conformers using the B3YLP/6-311G(d,p)/SMD_{1,4}-dioxane level of theory. Conformational analysis was carried out by varying the dihedral angle between the benzothiazole ring and the phenyl ring in steps of 30° over one complete rotation (0–360°). As a result, 12 conformers were identified, among which 2 were energetically more stable than others. These two conformers were found at 0° and 180°, with a total energy of −0.084752 Hartree. The plot of the scan coordinate versus total energy is shown in Figure 1. All the derivatives 1–5 mainly consisted of 2-aminobenzothiazole and the phenyl ring, and conformational analysis was carried out by varying the dihedral angle equal to 1. It was observed that the scanning result of compounds 2–5 exhibited the same behavior as compound 1.

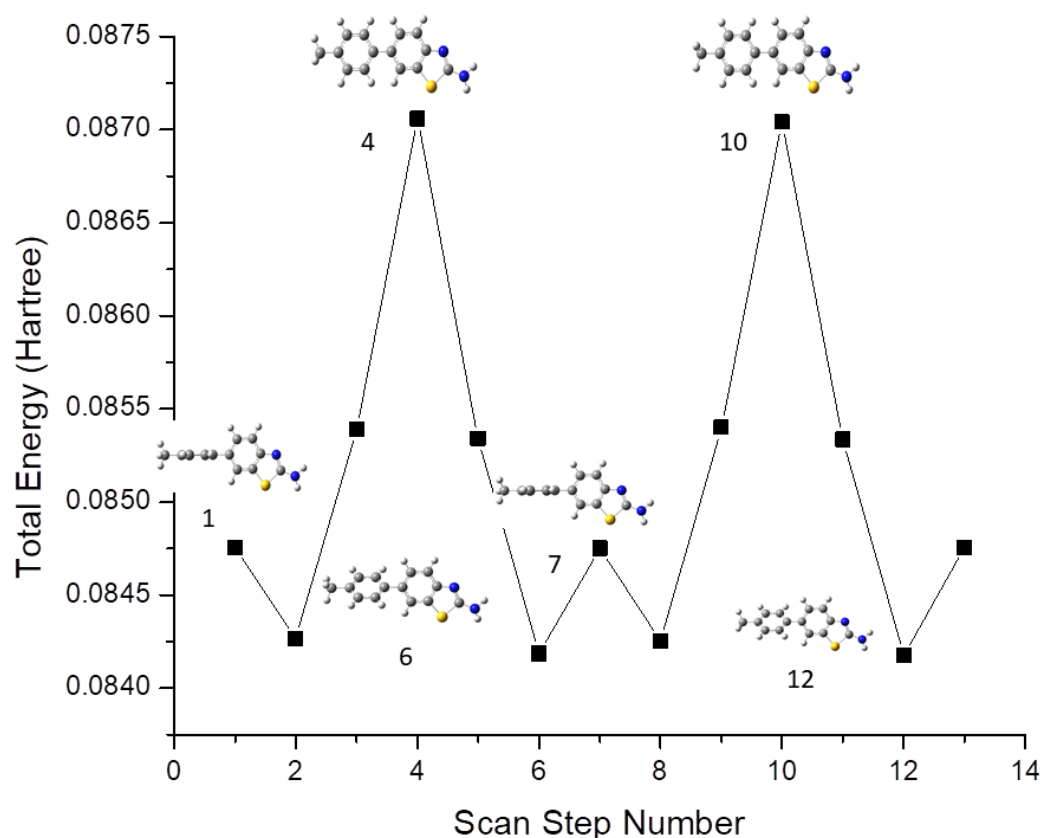


Figure 1. Theoretically calculated conformers of Compound 1 at B3YLP/6-311G(d,p)/SMD_{1,4}-dioxane level of theory.

3.2. Geometrical Parameters

Molecular geometry has always been an important part of the scientific method for studying complex molecules that require simplification to determine their characteristics. Molecular modeling provides a useful framework for the chemical realm that has applications both in the early and latter stages of scientific studies [23]. All the optimized structures of the studied benzothiazole derivatives are given in Figure 2. The geometrical parameters, such as bond lengths and bond angles, are calculated by applying the same level of theory

as in the optimizations. The selected bond lengths, bond angles and dihedral angles of 1 to 5 are given in Table 1. Most of the calculated geometrical parameters, such as bond lengths, bond angles and dihedral angles for all derivatives, have nearly the same values. It could be seen from Table 1 that the bonds C_7-C_{7a} and $C_{3a}-C_4$ of all the benzothiazole rings are shorter in comparison to the $C_{7a}-C_{3a}$ bonds of the respective rings. Interestingly, it is evident from Table 1 that the presence of different groups on the aromatic ring bound to benzothiazole does not change the geometry noticeably, as these groups are far from the benzothiazole moiety.

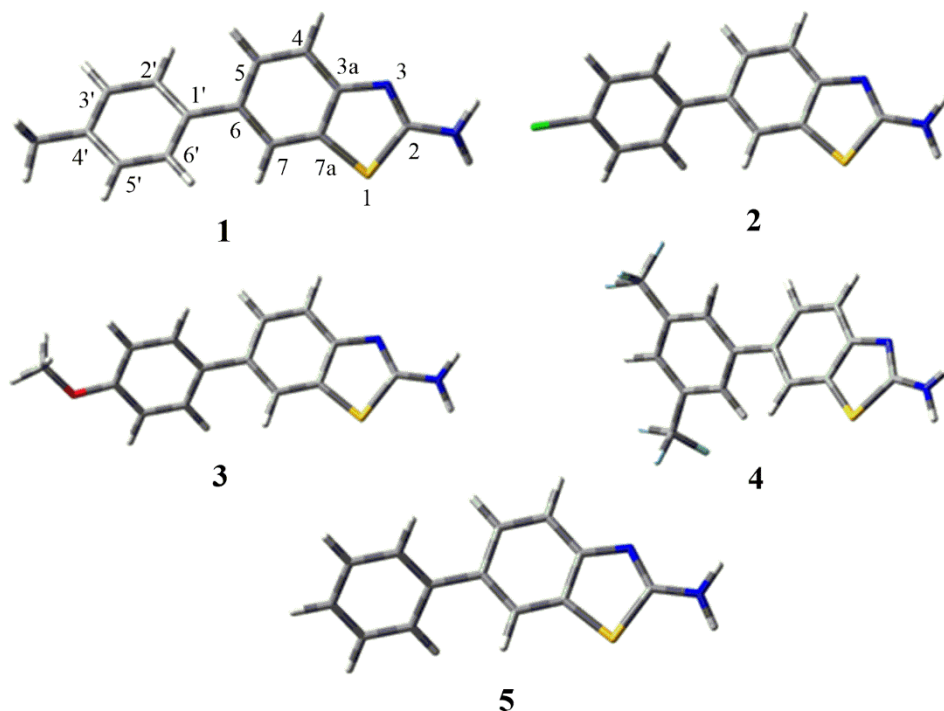


Figure 2. Optimized geometries of benzothiazole derivatives 1 to 5.

Table 1. Selected bond lengths, bond angles and dihedral angles of 1 to 5.

	Compounds				
	1	2	3	4	5
Bond lengths					
S_1-C_2	1.79	1.79	1.79	1.79	1.79
C_2-N_3	1.29	1.29	1.29	1.29	1.29
C_2-NH_2	1.36	1.35	1.36	1.35	1.36
N_3-C_{3a}	1.38	1.38	1.38	1.38	1.38
$C_{3a}-C_4$	1.39	1.39	1.39	1.39	1.39
C_7-C_{7a}	1.38	1.38	1.38	1.38	1.38
$C_{7a}-C_{3a}$	1.41	1.41	1.41	1.41	1.41
$C_{7a}-S_1$	1.76	1.76	1.76	1.76	1.76
$C_6-C_{1'}$	1.48	1.48	1.48	1.48	1.48
$C_{1'}-C_{2'}$	1.40	1.40	1.39	1.40	1.40

Table 1. Cont.

	Compounds				
	1	2	3	4	5
Bond angles					
S ₁ -C ₂ -N ₃	115.83	115.82	115.80	115.83	115.82
S ₁ -C ₂ -NH ₂	119.56	119.64	119.51	119.58	119.53
H ₂ N-C ₂ -N ₃	124.52	124.45	124.58	124.50	124.56
C ₂ -N ₃ -C _{3a}	111.21	111.22	111.22	111.19	111.22
N ₃ -C _{3a} -C _{7a}	115.91	115.92	115.90	115.92	115.90
C _{3a} -C _{7a} -S ₁	109.10	109.10	109.10	109.17	109.12
C _{7a} -S ₁ -C ₂	87.91	87.91	87.93	87.86	87.91
C ₅ -C ₆ -C _{1'}	120.89	120.81	120.97	120.81	120.85
C ₇ -C ₆ -C _{1'}	120.43	120.38	120.46	120.20	120.41
Dihedral angles					
S ₁ -C ₂ -N ₃ -C _{3a}	-0.01	-0.10	-0.11	0.08	-0.19
S ₁ -C ₂ -N-H	26.08	24.56	27.10	23.95	25.96
C ₂ -N ₃ -C _{3a} -C _{7a}	-0.08	-0.60	-0.77	-0.58	-0.67
N ₃ -C _{3a} -C _{7a} -S ₁	0.14	1.01	1.27	0.79	1.21
C _{3a} -C _{7a} -S ₁ -C ₂	-0.11	-0.83	-1.04	-0.58	-1.03
C _{7a} -S ₁ -C ₂ -NH ₂	177.03	177.60	177.48	177.34	177.65

3.3. Frontier Molecular Orbitals

Nowadays, the analysis of FMOs has become a very significant method for the explanation of the electronic characteristics and reactivity of compounds. The transfer of electrons from the ground to the excited state mainly takes place from the frontier molecular orbitals, and one can also explain the kinetic stability and reactivity of the compounds from the energy difference of HOMO and LUMO (ΔE). If ΔE is high, the compound is kinetically more stable and less reactive. If ΔE is low, then electrons can easily move from HOMO to LUMO, which makes the compound kinetically less stable and more reactive [24]. The energies of HOMO-LUMO, energy gap in HOMO-LUMO (ΔE), polarizability and hyperpolarizability of the studied compounds are given in Table 2. The values of ΔE of all studied benzothiazoles were in the range 4.46–4.73 eV. It was observed that compound **4** consisted of two -CF₃ moieties over both meta positions of the phenyl group that were further attached to benzothiazole and had the lowest ΔE value of 4.46 eV. So, it was the least stable compound among the series. Compounds **1** and **5** consisted of para methyl phenyl and phenyl, which were attached to the benzothiazole and had the highest ΔE values 4.71 eV and 4.73 eV, respectively, which rendered them the most stable and least reactive compounds. Compounds **2** and **3** consisted of para chlorophenyl and para methoxy phenyl that were attached to the benzothiazole ring and had intermediate energy gap (ΔE) values 4.62 eV and 4.64 eV, respectively. The strongly electron-withdrawing CF₃ groups in compound **4** made its ΔE smaller, thus making it the most reactive one in the series.

Table 2. Energies of HOMO-LUMO, HOMO-LUMO gap (ΔE) and hyperpolarizability values. The unit of β_0 is Hartree.

Compounds	E _{HOMO} (eV)	E _{LUMO} (eV)	ΔE (eV)	Hyperpolarizability (β_0) (Hartree)
1	-5.63	-0.92	4.71	1200.67
2	-5.78	-1.16	4.62	1989.38
3	-5.46	-0.82	4.64	153.51
4	-5.99	-1.53	4.46	3825.91
5	-5.71	-0.98	4.73	2031.01

The energy gap was decreased in the following order.

$$5 > 1 > 3 > 2 > 4$$

The FMOs maps were almost the same for all the studied compounds, except **4** in the benzothiazole series, which was slightly affected due to the presence of two CF₃ groups attached to the meta position of the phenyl ring. The frontier molecular orbitals are shown in Figure 3.

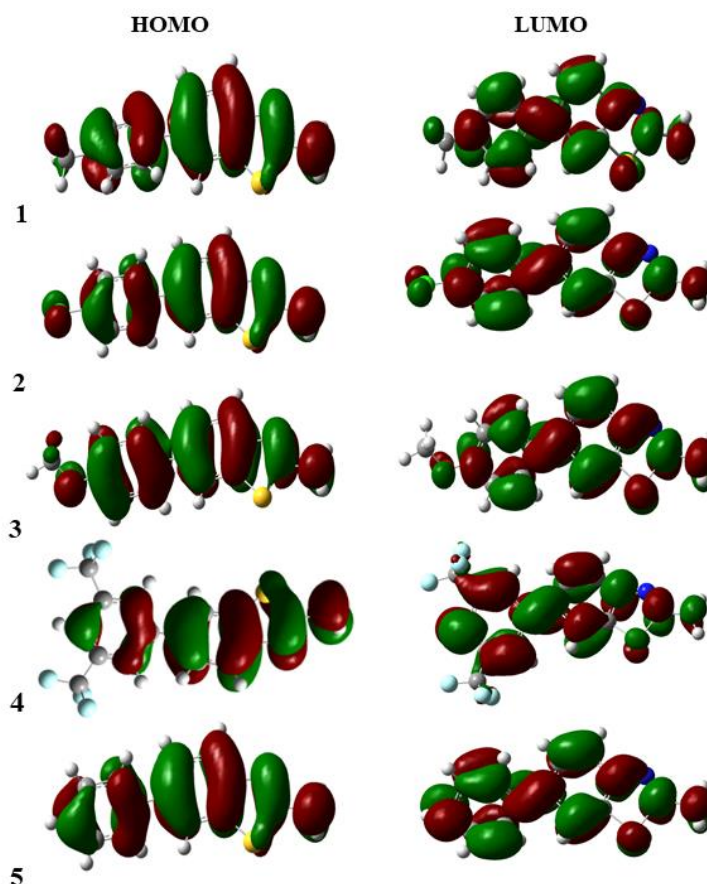


Figure 3. Frontier molecular orbitals of 1–5.

3.4. NLO Properties

The use of organic compounds in optoelectronics has increased melodramatically, and the increasing volume of communication and information processing is continuing to be a big challenge in the up-to-date technology [25]. The NLO properties of the compounds were calculated, and the hyperpolarizability values are given in Table 2. The substituted molecule **4** with CF₃ group at the *m* position had the highest hyperpolarizability value, i.e., 3825.91 Hartree, and **3**, substituted with –OCH₃ at *p* position, had the lowest hyperpolarizability value of 153.51 Hartree.

Hyperpolarizability decreased in the following order.

$$4 > 5 > 2 > 1 > 3$$

The molecules with high hyperpolarizability had a high NLO response, and the molecules with low hyperpolarizability had a low NLO response. In the literature, the theoretically calculated hyperpolarizability value of 2(3H)-benzothiazolone was reported as 505.4 Hartree.

3.5. Molecular Electrostatic Potential (MEP)

The electron density can be displayed by MEP, and it is a very useful method for finding the positions of nucleophilic and electrophilic reactions and hydrogen bonding [26]. MEP is a three-dimensional graph that can be used to show the charge distribution and properties

related to the charge of compounds. It gives a graphical understanding of the relative polarity of molecules. MEP yields information about molecular regions that are preferred or avoided by electrophiles or nucleophiles. Any chemical system creates an electrostatic potential around itself. When a hypothetical “volumeless” unit of positive charge is used as a probe, it experiences attractive or repulsive forces in regions where the electrostatic potential is negative or positive, respectively. In the MEP maps, the red color shows the electron-rich site, which relates to electrophilic reactivity, while the blue color shows the electron-deficient site, which relates to nucleophilic reactivity, as shown in Figure 4.

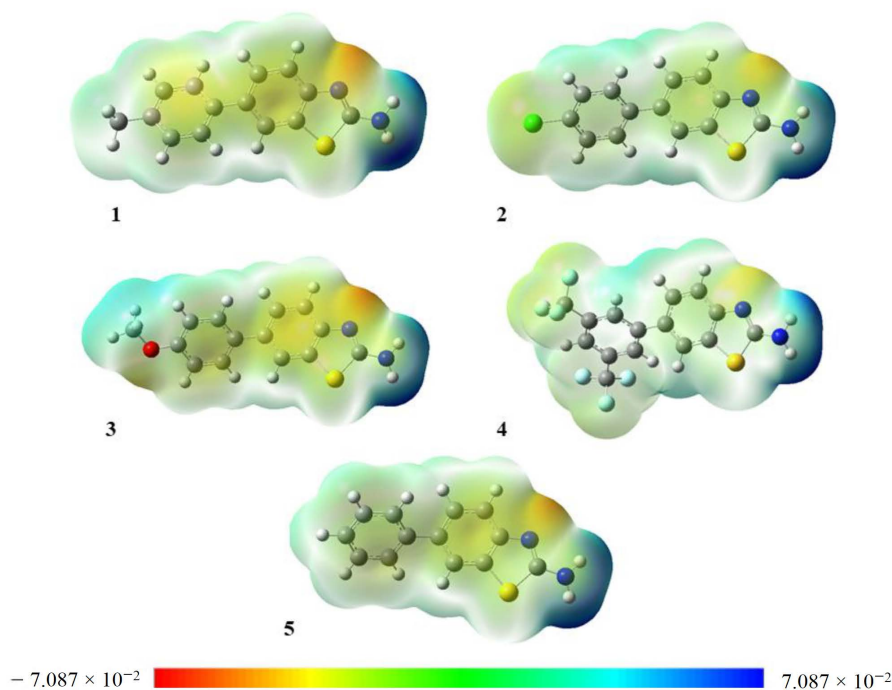


Figure 4. Molecular electrostatic potential maps of 1–5 plotted using iso value = 0.0004. Units of the scale of electron charge density are Hartree.

3.6. Density of States

The density of states (DOS) was determined using the GaussSum package, which gives the molecular orbital contributions of different essential elements for the entire system of the compound [27], and the corresponding DOS of 1 is shown in Figure 5. The DOS spectra of the remaining molecules are given in Figures S6–S9 (see in Supplementary Materials). The blue and green lines in the DOS spectrum show the levels of HOMO and LUMO. The spatial redistribution of the frontier orbital is a three-dimensional representation of the local density of states, which visually shows the electron density of the molecule [28]. The variation of the HOMO-LUMO gap can be confirmed with the DOS spectrum [29]. This spectrum is used to determine how many positions are accessible at a specific energy position. The starting lines at the energy axis of the graph, which run from -20 eV to $-eV$, are known as occupied, filled and donor orbital, and from -5 eV to 5 eV, they are known as virtual, unfilled and acceptor orbital. At a particular energy level, the high intensity of DOS shows that many positions are accessible for occupation. Zero intensity of DOS depicts that no states are available for occupation by the system.

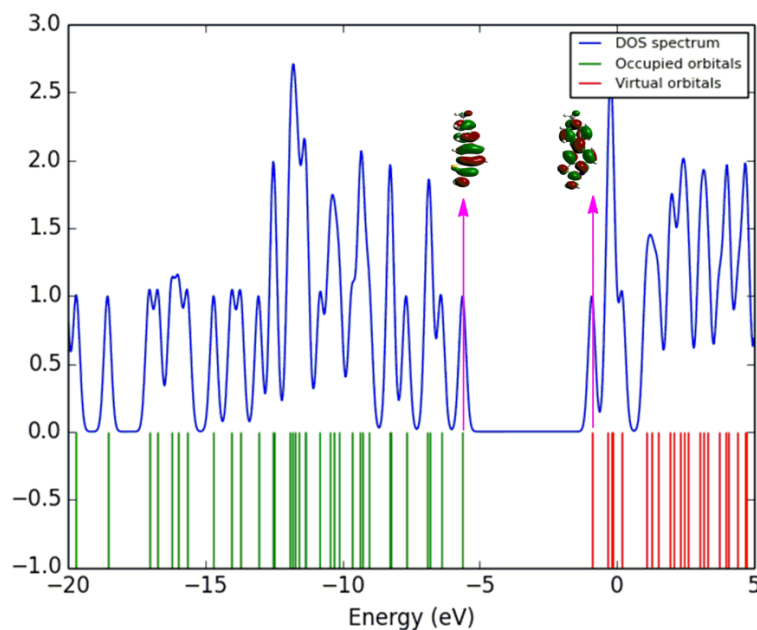


Figure 5. DOS spectrum of **1** visualized using GaussSum.

3.7. NMR Spectra

NMR spectroscopy has proven to be an excellent tool for clarifying the structure and molecular conformations. Facts have proved that the GIAO method [30] has been accurate and widely accepted. DFT shielding calculation is fast and suitable for large systems. To provide a clear analysis and assignment of the ^{13}C and ^1H NMR spectra, the chemical shift of ^{13}C and ^1H of the studied compounds was calculated using the GIAO method at the B3LYP/6-311G(d,p)/SMD_{Chloroform} level of theory [31]. The calculated chemical shift of ^1H of all the proton of the aromatic ring ranged from 7.90 to 7.15 ppm, which resembles experimental values of 7.70–7.25 ppm, except for compound **4** in which the protons of the phenyl group were in the range of 8.22–8.05 ppm, and experimental values were also between 8.22 and 8.08 ppm. The theoretical calculated chemical shift values of ^1H and ^{13}C -NMR are given in Table 3. A comparison of the calculated and experimental chemical shift values is also provided in Table S1 in the Supplementary Materials.

Table 3. The chemical shifts of ^1H and ^{13}C -NMR calculated with the GIAO method at the B3LYP/6-311G (d,p)/SMD_{Chloroform} level of theory.

Position of H-Atom	Compounds				
	1	2	3	4	5
4	7.68	7.67	7.66	7.74	7.90
5	7.58	7.55	7.54	7.69	7.59
7	7.87	7.87	7.85	7.98	7.69
2'	7.64	7.65	7.67	8.22	7.68
3'	7.51	7.52	6.92	–	7.66
4'	–	–	–	8.05	7.53
5'	7.50	7.52	7.17	–	7.66
6'	7.58	7.60	7.60	8.16	7.73

Table 3. Cont.

Position of H-Atom	Compounds				
	1	2	3	4	5
Position of C-Atom					
C ₂	170.5	170.9	170.6	171.5	170.8
C _{3a}	155.7	156.4	155.2	157.3	155.9
C ₄	122.6	122.7	122.6	123.1	122.7
C ₅	129.4	129.4	128.9	129.6	129.6
C ₆	141.8	139.9	141.6	137.9	141.8
C ₇	123.2	123.3	122.8	123.8	123.5
C _{7a}	141.9	141.9	141.9	142.3	141.8
C _{1'}	145.1	146.9	139.2	149.9	148.3
C _{2'}	131.6	133.1	132.8	133.8	131.8
C _{3'}	133.1	133.0	111.7	136.3	132.6
C _{4'}	143.0	144.9	149.2	124.3	130.6
C _{5'}	133.1	133.0	120.9	136.1	132.6
C _{6'}	131.4	133.8	132.7	133.1	131.5

3.8. UV-Visible Spectra

The light energy is used to transfer electrons from the lower state to the higher state. When the absorption of light is measured according to the frequency or wavelength of the light, the spectrum can be obtained. Electron-bearing molecules in delocalized aromatic systems generally absorb light in the near-ultraviolet (150–400 nm) or visible (400–800 nm) region [32]. The absorption wavelengths (λ_{\max}), oscillator strengths (f) and excitation energies (E) are given in Table 4. The UV-visible spectrum of compounds 1 to 5 is shown in Figure 6. Because of the similar chromophore, the UV spectra of all the compounds are quite similar.

Table 4. Theoretically calculated absorption wavelengths (λ_{\max}), oscillator strengths (f) and excitation energies (E) of all the studied compounds. The abbreviations ES1, ES2 and ES3 indicate the first, second and third excitation energies.

Compounds	Major Contribution	λ_{\max} (nm)	Oscillator Strengths (f)	Excitation Energies (eV)
1	(ES1) H → L 70%	382.25	0.2735	3.24
	(ES2) H → L 60%	265.23	0.0033	4.67
	(ES3) H → L 66%	247.58	0.0431	5.007
2	(ES1) H → L 69%	383.06	0.2773	3.23
	(ES2) H → L 67%	330.41	0.0423	3.75
	(ES3) H → L 67%	301.83	0.0195	4.10
3	(ES1) H → L 69%	382.55	0.2750	3.24
	(ES2) H → L 67%	330.92	0.0424	3.74
	(ES3) H → L 67%	301.29	0.0189	4.11
4	(ES1) H → L 69%	384.48	0.2729	3.22
	(ES2) H → L 66%	330.32	0.0411	3.75
	(ES3) H → L 69%	311.23	0.0051	3.98
5	(ES1) H → L 69%	382.35	0.2691	3.24
	(ES2) H → L 67%	331.06	0.0424	3.74
	(ES3) H → L 67%	301.11	0.0192	4.11

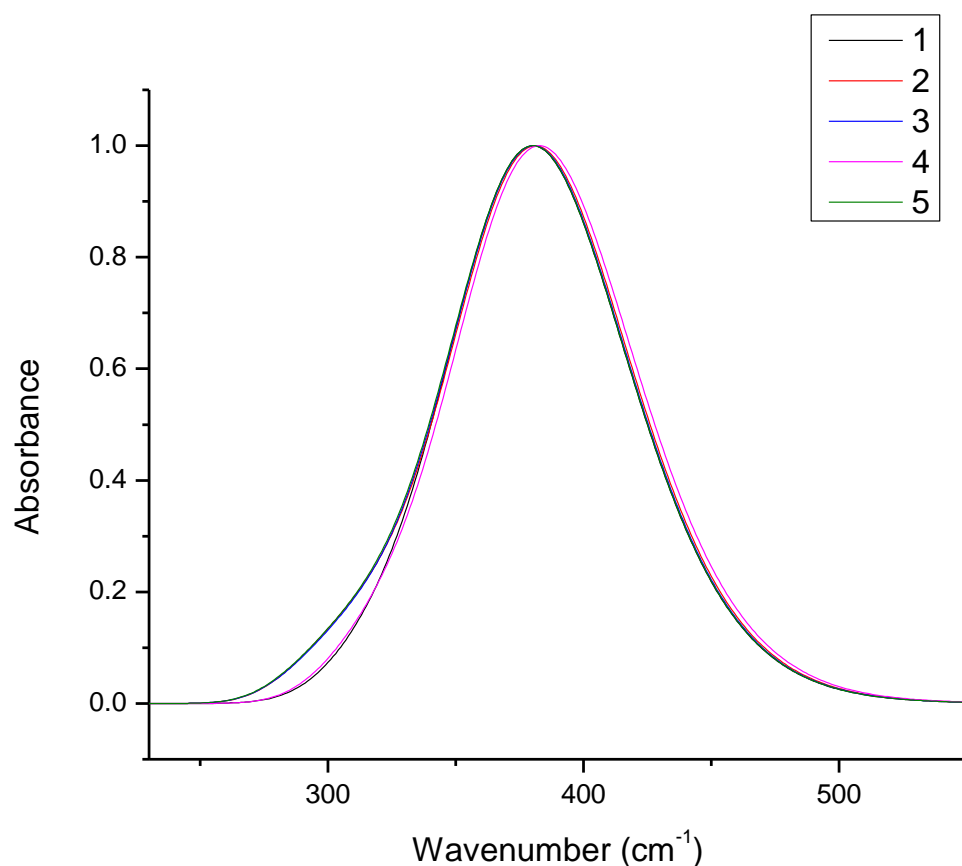


Figure 6. UV-visible spectra of 1 to 5.

3.9. IR Spectra

The IR spectra of the studied compounds were not studied experimentally or theoretically in the literature. Therefore, the vibrational spectra of these benzothiazole derivatives were computed. The IR spectrum of compound **1** is shown in Figure 7, and the remaining IR spectra are given in Figures S2–S5 (see in Supplementary Materials). None of the calculated vibrational spectra had any imaginary frequency, and the theoretically calculated vibrational frequency ranges and modes of **1** to **5** are given in Table 5.

Amines have a very strong tendency to self-associate by hydrogen bonding and absorption bands depending on the nature of the sample. The amino group at position 2 shows absorption band 1 is between 3680 and 3690 cm^{-1} , and the other is between 3566 and 3572 cm^{-1} , arising, respectively, from the scissoring and rocking vibrations in **2** to **5**. However, in the case of **1**, the amino group at position 2 shows two absorption bands—one at 3681 cm^{-1} and the other at 3566 cm^{-1} —but vibrations modes are antisymmetric and symmetrically stretched. The absorption bands of the H–N–H groups are in the 1590–1700 and 1300–1320, 1100–1200 cm^{-1} regions, with antisymmetric and symmetric stretching vibrations, respectively. The absorption bands of C–H in phenyl ring deformation vibrations are observed in the range of 3150–3262, 1320–1520, 1100–1210–800–985 cm^{-1} . The absorption bands of C–H in methyl group deformation vibrations are observed in the range of 3008–3132 cm^{-1} . The stretching absorption bands of C–CF₃ and C–F appear at 1382 and 1119 cm^{-1} . The stretching absorption bands of C–OCH₃ and O–CH₃ are observed at 1279 and 1059 cm^{-1} . The characteristic stretching vibration of the C–C of phenyl and benzo ring appear in the 600–795 cm^{-1} frequency range. The observed stretching vibrations range of C–NH₂ is 620–640 cm^{-1} in all benzothiazole derivatives, except **1**.

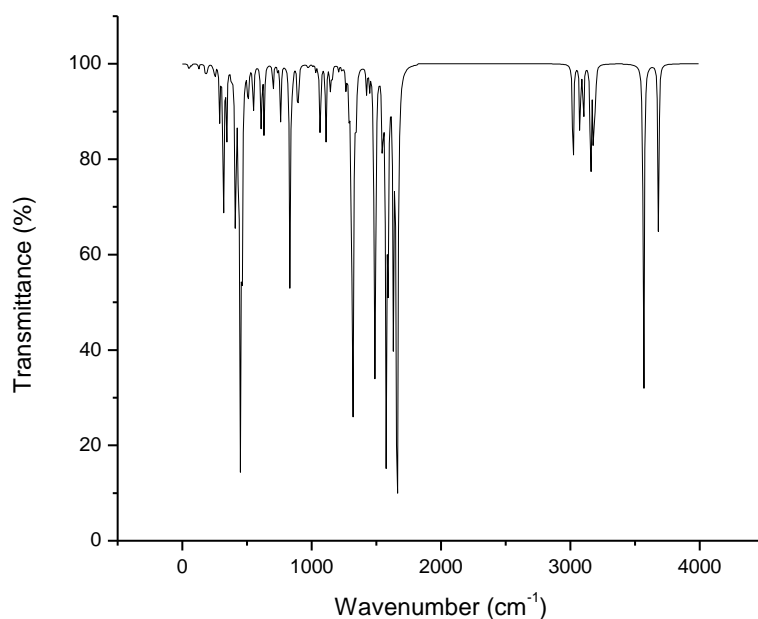


Figure 7. IR spectrum of 1.

Table 5. Theoretically calculated vibrational frequencies and vibrational modes of 1 to 5.

Compounds					Bond/Groups	Vibrational Modes
1	2	3	4	5		
–	3680	3686	3690	3682	NH ₂ (amine)	Scissoring
–	3568	3570	3568	3572	NH ₂ (amine)	Rocking
3681	–	–	–	–	NH ₂ (amine)	Antisymmetric Stretching
3566	–	–	–	–	NH ₂ (amine)	Antisymmetric Stretching
3230	3240	3226	3165	3330	C–H (phenyl)	Deformation
3155	3165	3170	3195	3150	C–H (phenyl)	Stretching
3132	–	–	–	–	C–H (methyl)	Deformation
3074	–	–	–	–	H–C–H (methyl)	Antisymmetric Stretching
3020	–	–	–	–	H–C–H (methyl)	Symmetric Stretching
1590	–	–	–	–	NH ₂ (amine)	Scissoring
1590	1645	1679	1700	1620	NH ₂ (amine)	Antisymmetric Stretching
1510	1560	1635	1660	1500	C–C (phenyl)	Stretching
1565	1590	1625	1650	1550	C–C (benzo)	Stretching
1490	–	–	–	–	H–C–H (methyl)	Deformation
1320	1460	1430	1530	1380	C–H (phenyl)	Deformation
–	–	–	1382	–	C–CF ₃	Stretching
1345	1390	1425	1490	1310	C–H (benzo)	Stretching
–	1310	1315	1325	1310	NH ₂ (amine)	Symmetric Stretching
–	–	1300	1320	–	C–N (benzo)	Stretching
–	1275	1265	1290	1260	C–H (benzo)	Stretching
–	–	1279	–	–	C–OCH ₃	Stretching
1260	–	–	–	–	C–H (benzo)	Deformation
–	1100	1115	1120	1105	NH ₂ (amine)	Symmetric Stretching
1110	–	–	–	–	NH ₂ (amine)	Deformation
1150	1155	1155	1160	1150	C–H (benzo)	Stretching
–	–	–	1119	–	C–F	Stretching
–	1099	–	–	–	C–Cl	Stretching
–	–	1059	–	–	O–CH ₃	Stretching
1020	1025	1035	1040	1015	C–C (phenyl)	Stretching
1055	1075	1075	1080	1060	C–C (benzo)	Stretching
8010	885	915	985	8025	C–H (phenyl)	Deformation

3.10. Reactivity Parameters

The reactivity parameters, such as chemical softness (σ), chemical hardness (η), electrophilicity index (ω), electronic chemical potential (μ), ionization potential (I) and electron affinity (A) are calculated from E_{HOMO} and E_{LUMO} , as per Equations (3)–(6) [33].

According to Koopman's theorem [34]

$$\text{Ionization potential} = -E_{\text{HOMO}} \quad (1)$$

$$\text{Electron affinity} = -E_{\text{LUMO}} \quad (2)$$

$$\eta = (E_{\text{HOMO}} - E_{\text{LUMO}})/2 \quad (3)$$

$$\mu = -(E_{\text{HOMO}} + E_{\text{LUMO}})/2 \quad (4)$$

$$\omega = \mu^2/2\eta \quad (5)$$

$$\sigma = 1/\eta \quad (6)$$

Chemical softness and hardness are the basic concepts called global reactivity parameters, which are calculated with the help of DFT. The softness and hardness can be predicted from the energy gap of the molecules. Large energy gap leads to a hard molecule, and small energy gap leads to a soft molecule [31]. In this series, compounds **1** and **5** have the highest energy gap (ΔE) and also the highest chemical hardness values of 2.35 eV and 2.36 eV, respectively, which lead to the most stable and least reactive compounds. Compound **4** has the lowest energy gap (ΔE) and also the lowest chemical hardness value of 2.35 eV, which leads it to being the least stable and most reactive compound. Compound **4** also has the highest ionization potential (5.98 eV) and electron affinity (1.53 eV). Chemical hardness can be easily associated with the substance's resistance to deformation, so the results are well in line with the ΔE values, as compounds **1** and **5** have the highest values of η , which supports the conclusion that they are the least reactive ones in the series. Ionization potential values of the subject compounds also provide useful information, as all the compounds contain a hydrogen-donor amine group and therefore have an ionizable basic center. This may also stabilize the extra charges received. The values of chemical softness (σ), chemical hardness (η), electrophilicity index (ω), electronic chemical potential (μ), ionization potential (I) and electron affinity (A) are given in Table 6.

Table 6. The values of reactivity parameters in eV of all the studied compounds (1–5).

Compounds	I	A	η	σ	μ	ω
1	5.62	0.91	2.35	0.42	−3.27	2.27
2	5.77	1.16	2.30	0.43	−3.47	2.61
3	5.46	0.81	2.32	0.43	−3.14	2.12
4	5.98	1.53	2.22	0.45	−3.76	3.17
5	5.70	0.97	2.36	0.42	−3.34	2.35

3.11. Molecular Docking Study

In this research, we are interested in studying the antibacterial effects of derivatives against distinct bacteria. The derivatives were subjected to molecular docking study. The protein structure was chosen from (*Klebsiella aerogenes*) (PDB ID: 2KAU) Gram-negative bacteria, whereas the docking results suggest that compound **3** exhibited the highest predicted affinity (−3.45 kcal/mol) as compared to others. ASP-329 residue of the protein structure illustrated hydrogen bonds with bond lengths of 1.64 Å and 1.73 Å with the amide group (NH) and the amino group (−NH₂) of compound **3**, respectively. The docking score, ΔG edvw, ΔG coulomb, ΔG energy, ΔG internal, ΔG model values of compound **3** are also lower in value than the rest of the molecules (Table 7). In comparison with thiourea, only ΔG coulomb, and ΔG internal are higher in value, and the rest of the calculated values show that compound **3** binding affinity is better with the 2KAU protein (Table 7).

Binding affinities with the formation of H-bonds and other non-bonding interactions of the complexes are presented in Figure 8.

Table 7. Binding energies (kcal/mol) of urease (PDB: 2KAU) with selected ligands 1 to 5.

Compounds	Docking Score	ΔG Edvw	ΔG Coloumb	ΔG Energy	ΔG Internal	ΔG Model
1	−2.71	−26.155	−0.429	−26.584	0.09	−34.161
2	−3.064	−25.524	−3.234	−28.758	0.189	−34.231
3	−3.45	−25.911	−4.781	−30.692	4.231	−36.37
4	−2.053	−30.72	−1.026	−31.747	0.952	−43.277
5	−2.416	−24.444	−1.118	−25.562	0.041	−32.142
Thiourea	−2.46	−6.481	−8.095	−14.576	0	−15.732

Binding Energies (kcal/mol) of <i>Staphylococcus aureus</i> bacterium (PDB: 7EL1)						
1	−3.345	−17.9	−4.783	−22.683	0.03	−27.757
2	−3.26	−19.708	−4.279	−23.986	0.028	−29.282
3	−3.309	−20.484	−4.307	−24.791	0.082	−30.202
4	−2.58	−19.34	−3.73	−23.069	0.227	−26.847
5	−2.844	−17.946	−2.751	−20.697	0.123	−24.357

Although the protein structure (PDB ID: 7EL1) from *Staphylococcus aureus* bacterium was also docked against the compounds, the docking results revealed that **1** exhibited the highest binding affinity (3.345 kcal/mol). Amino acid Glu-378 charged negative residues displayed H-bonds with bond length of 1.74 Å to the amino group of inhibitors. The ΔG edvw, ΔG energy, ΔG internal, ΔG model values of compound **3** are also lower in value than the rest of the molecules (Table 7). The docking score and ΔG coloumb of compound **1** is slightly better than compound **3**. In comparison with thiourea, all values are better for compound **3**, and the rest of the calculated values show that compound **3** binding affinity is better with the 7EL1 protein (Table 7). In addition, other residues of structure contact ligand via distinct interactions are mentioned in Figure 9. We may infer that **1** and **3** exhibit good binding energies and explore H-bonds in the residues of structures that can be used to establish new therapies against different diseases.

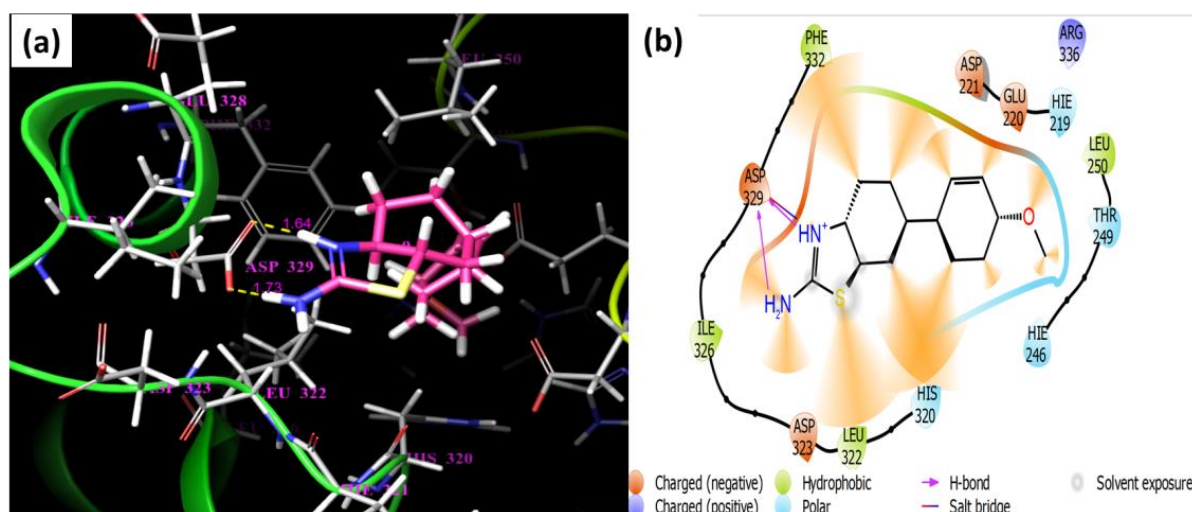


Figure 8. (a) Schematic diagram of protein and ligand **3** depicts three-dimensional complex, while (b) depicts two-dimensional interactions of the protein and ligand. Hydrogen bonds, as well as other interactions, are displayed in the two-dimensional figure.

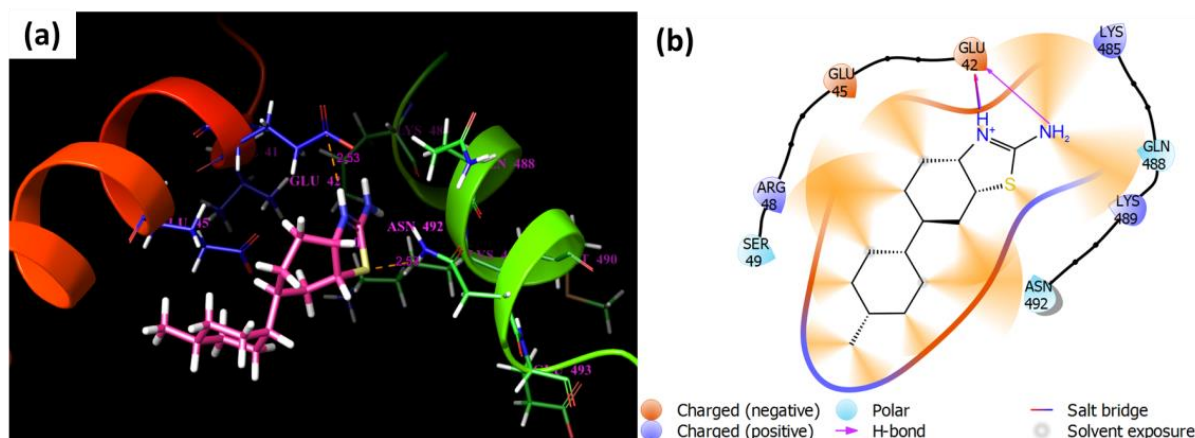


Figure 9. (a). Molecular docking of 7EL1 with ligand 1. (b). Two-dimensional structure, hydrogen bonds, hydrophobic and other interactions.

4. Conclusions

The vibrational frequencies, thermodynamic properties, structural properties and optimized geometry of the studied benzothiazole derivatives were reported by applying the DFT method. The energy difference between the HOMO and LUMO elucidated the consequent electronic transition taking place within the molecule, particularly from the benzothiazole group to the amino group. Moreover, the polarizability and hyperpolarizability values of the molecule elucidated that compound **4** is an interesting agent for further studies of NLO properties. The reactivity parameters of the studied compounds, such as ionization energy, electron affinity, chemical potential electrophilicity, softness and hardness, were calculated by using the same DFT methods. According to the reactivity parameters, compounds **1** and **5** were kinetically the most stable, while compound **4** was the most reactive one. The protein structure was chosen from *Klebsiella aerogenes* (PDB ID: 2KAU) Gram-negative bacteria. The docking results suggest that **3** exhibited the highest predicted affinity (-3.45 kcal/mol) as compared to others.

Supplementary Materials: The following supporting information can be downloaded at: <https://www.mdpi.com/article/10.3390/cryst12070912/s1>, Figure S1: Structure with IUPAC names of Benzothiazole derivatives; Figure S2: IR spectrum of **2**; Figure S3: IR spectrum of **3**; Figure S4: IR spectrum of **4**; Figure S5: IR spectrum of **5**; Figure S6: DOS Spectrum of **2** calculated from GaussSum; Figure S7: DOS Spectrum of **3** calculated from GaussSum; Figure S8: DOS Spectrum of **4** calculated from GaussSum; Figure S9: DOS Spectrum of **5** calculated from GaussSum; Table S1: Chemical shifts of ^1H and ^{13}C -NMR calculated.

Author Contributions: Conceptualization, N.R. and M.A.H.; methodology, A.M. and N.R., software, A.M., M.A.H. and S.M. (Sadaf Mutahir); validation, G.A.A., N.R., S.M. (Sajid Mahmood) and M.A.; formal analysis, M.A., K.G.A., M.B., A.M., S.M. (Sajid Mahmood) and N.R.; investigation, A.M. and S.M. (Sajid Mahmood); resources, N.R., M.N.A. and G.A.A.; data curation, M.B., N.R. and K.G.A.; writing—original draft preparation, A.M., G.A.A., M.B. and S.M. (Sadaf Mutahir); writing—review and editing, A.M., M.B., K.G.A. and G.A.A. visualization, A.M., S.M. (Sadaf Mutahir) and S.M. (Sajid Mahmood); supervision, N.R. and M.A.H.; project administration, N.R. All authors have read and agreed to the published version of the manuscript.

Funding: This research was funded by project ZC304021910.

Acknowledgments: The data reported herein are part of the M. Phil thesis research work of Adeel Mubarik.

Conflicts of Interest: There are no conflicts of interest.

References

1. Sathyanarayananmoorthi, V.; Karunathan, R.; Kannappan, V. Molecular modeling and spectroscopic studies of Benzothiazole. *J. Chem.* **2013**, *2013*, 258519. [[CrossRef](#)]
2. Giorgioni, G.; Accorroni, B.; Di Stefano, A.; Marucci, G.; Siniscalchi, A.; Claudi, F. Benzimidazole, Benzoxazole and Benzothiazole Derivatives as 5HT 2B Receptor Ligands. Synthesis and Preliminary Pharmacological Evaluation. *Med. Chem. Res.* **2005**, *14*, 57–73. [[CrossRef](#)]
3. Gull, Y.; Rasool, N.; Noreen, M.; Altaf, A.A.; Musharraf, S.G.; Zubair, M.; Nasim, F.-U.-H.; Yaqoob, A.; DeFeo, V.; Zia-Ul-Haq, M. Synthesis of N-(6-Arylbenzo[d]thiazole-2-acetamide derivatives and their biological activities: An experimental and computational approach. *Molecules* **2016**, *21*, 266. [[CrossRef](#)] [[PubMed](#)]
4. Paramashivappa, R.; Kumar, P.P.; Rao, P.S.; Rao, A.S. Design, synthesis and biological evaluation of benzimidazole/benzothiazole and benzoxazole derivatives as cyclooxygenase inhibitors. *Bioorg. Med. Chem. Lett.* **2003**, *13*, 657–660. [[CrossRef](#)]
5. Mahran, M.A.; William, S.; Ramzy, F.; Sembel, A.M. Synthesis and in vitro evaluation of new benzothiazole derivatives as schistosomicidal agents. *Molecules* **2007**, *12*, 622–633. [[CrossRef](#)]
6. Rajeeva, B.; Srinivasulu, N.; Shantakumar, S. Synthesis and Antimicrobial Activity of Some New 2-Substituted Benzothiazole Derivatives. *E-J. Chem.* **2009**, *6*, 775–779. [[CrossRef](#)]
7. Kini, S.; Swain, S.; Gandhi, A. Synthesis and evaluation of novel benzothiazole derivatives against human cervical cancer cell lines. *Indian J. Pharm. Sci.* **2007**, *69*, 46. [[CrossRef](#)]
8. Kaur, H.; Kumar, S.; Singh, I.; Saxena, K.; Kumar, A. Synthesis, characterization and biological activity of various substituted benzothiazole derivatives. *Dig. J. Nanomater. Bios.* **2010**, *5*, 67–76.
9. Vicini, P.; Geronikaki, A.; Incerti, M.; Busonera, B.; Poni, G.; Cabras, C.A.; La Colla, P. Synthesis and biological evaluation of benzo[d]isothiazole, benzothiazole and thiazole Schiff bases. *Bioorg. Med. Chem.* **2003**, *11*, 4785–4789. [[CrossRef](#)]
10. Yadav, P.; Devprakash, D.; Senthilkumar, G. Benzothiazole: Different methods of synthesis and diverse biological activities. *ChemInform* **2011**, *42*. [[CrossRef](#)]
11. Netalkar, P.P.; Netalkar, S.P.; Budagumpi, S.; Revankar, V.K. Synthesis, crystal structures and characterization of late first row transition metal complexes derived from benzothiazole core: Anti-tuberculosis activity and special emphasis on DNA binding and cleavage property. *Eur. J. Med. Chem.* **2014**, *79*, 47–56. [[CrossRef](#)] [[PubMed](#)]
12. Thakkar, S.S.; Thakor, P.; Ray, A.; Doshi, H.; Thakkar, V.R. Benzothiazole analogues: Synthesis, characterization, MO calculations with PM6 and DFT, in silico studies and in vitro antimalarial as DHFR inhibitors and antimicrobial activities. *Bioorg. Med. Chem.* **2017**, *25*, 5396–5406. [[CrossRef](#)] [[PubMed](#)]
13. Bondock, S.; Fadaly, W.; Metwally, M. Recent trends in the chemistry of 2-aminobenzothiazoles. *J. Sulphur Chem.* **2009**, *30*, 74–107. [[CrossRef](#)]
14. Lewars, E. Computational chemistry. In *Introduction to the Theory and Applications of Molecular and Quantum Mechanics*; Springer: Berlin/Heidelberg, Germany, 2003; p. 318.
15. Ramachandran, K.; Deepa, G.; Namboori, K. *Computational Chemistry and Molecular Modeling: Principles and Applications*; Springer Science & Business Media: Berlin/Heidelberg, Germany, 2008.
16. Gull, Y.; Rasool, N.; Noreen, M.; Nasim, F.-u.-H.; Yaqoob, A.; Kousar, S.; Rashid, U.; Bukhari, I.H.; Zubair, M.; Islam, M. Efficient synthesis of 2-amino-6-arylbenzothiazoles via Pd (0) Suzuki cross coupling reactions: Potent urease enzyme inhibition and nitric oxide scavenging activities of the products. *Molecules* **2013**, *18*, 8845–8857. [[CrossRef](#)]
17. Hashmi, M.A.; Khan, A.; Ayub, K.; Farooq, U. Spectroscopic and density functional theory studies of 5, 7, 3', 5'-tetrahydroxyflavanone from the leaves of *Olea ferruginea*. *Spectrochim. Acta Part A Mol. Biomol. Spectrosc.* **2014**, *128*, 225–230. [[CrossRef](#)]
18. Mubarik, A.; Rasool, N.; Hashmi, M.A.; Mansha, A.; Zubair, M.; Shaik, M.R.; Sharaf, M.A.; Awwad, E.M.; Abdelgawad, A. Computational Study of Structural, Molecular Orbitals, Optical and Thermodynamic Parameters of Thiophene Sulfonamide Derivatives. *Crystals* **2021**, *11*, 211. [[CrossRef](#)]
19. Ahmad, G.; Rasool, N.; Mubarik, A.; Zahoor, A.F.; Hashmi, M.A.; Zubair, M.; Bilal, M.; Hussien, M.; Akhtar, M.S.; Haider, S. Facile Synthesis of 5-Aryl-N-(pyrazin-2-yl) thiophene-2-carboxamides via Suzuki Cross-Coupling Reactions, Their Electronic and Nonlinear Optical Properties through DFT Calculations. *Molecules* **2021**, *26*, 7309. [[CrossRef](#)]
20. Liu, H.; Zhu, Y.; Lu, Z.; Huang, Z. Structural basis of *Staphylococcus aureus* Cas9 inhibition by AcrIIA14. *Nucleic Acids Res.* **2021**, *49*, 6587–6595. [[CrossRef](#)]
21. Jabri, E.; Carr, M.B.; Hausinger, R.P.; Karplus, P.A. The crystal structure of urease from *Klebsiella aerogenes*. *Science* **1995**, *268*, 998–1004. [[CrossRef](#)]
22. Bhachoo, J.; Beuming, T. Investigating protein–peptide interactions using the Schrödinger computational suite. In *Modeling Peptide-Protein Interactions*; Springer: Berlin/Heidelberg, Germany, 2017; pp. 235–254.
23. Lu, J.; Sigalovsky, D.; Hango, C.R.; Devaney, K.J. Computational Chemistry in the High School Classroom. Ph.D. Thesis, Worcester Polytechnic Institute, Worcester, MA, USA, 2014.
24. Mahmood, N.; Rasool, N.; Ikram, H.M.; Hashmi, M.A.; Mahmood, T.; Zubair, M.; Ahmad, G.; Rizwan, K.; Rashid, T.; Rashid, U. Synthesis of 3, 4-Biaryl-2, 5-Dichlorothiophene through Suzuki Cross-Coupling and Theoretical Exploration of Their Potential Applications as Nonlinear Optical Materials. *Symmetry* **2018**, *10*, 766. [[CrossRef](#)]
25. Shen, Y.-R. *The Principles of Nonlinear Optics*; OSTI: Oak Ridge, TN, USA, 1984.

26. Politzer, P.; Truhlar, D.G. *Chemical Applications of Atomic and Molecular Electrostatic Potentials: Reactivity, Structure, Scattering, and Energetics of Organic, Inorganic, and Biological Systems*; Springer Science & Business Media: Berlin/Heidelberg, Germany, 2013.
27. Pandey, U.; Srivastava, M.; Singh, R.; Yadav, R. DFT study of conformational and vibrational characteristics of 2-(2-hydroxyphenyl) benzothiazole molecule. *Spectrochim. Acta Part A Mol. Biomol. Spectrosc.* **2014**, *129*, 61–73. [[CrossRef](#)] [[PubMed](#)]
28. Xie, B.; Wang, Q.; Long, X.; Hu, S.; Gao, T. Density Function Theory Study on the Reaction Mechanism of Cerium with Oxygen for Ce-bearing Aerosol Particle Formation. *J. Wuhan Univ. Technol. Sci. Ed.* **2020**, *35*, 501–505. [[CrossRef](#)]
29. Magyar, R.; Tretiak, S.; Gao, Y.; Wang, H.-L.; Shreve, A. A joint theoretical and experimental study of phenylene–acetylene molecular wires. *Chem. Phys. Lett.* **2005**, *401*, 149–156. [[CrossRef](#)]
30. Siehl, H.U.; Müller, T.; Gauss, J. NMR Spectroscopic and quantum chemical characterization of the (E)– and (Z)– isomers of the penta-1, 3-dienyl-2-cation. *J. Phys. Org. Chem.* **2003**, *16*, 577–581. [[CrossRef](#)]
31. Xavier, R.J.; Dinesh, P. Spectroscopic (FTIR, FT-Raman, ¹³C and ¹H NMR) investigation, molecular electrostatic potential, polarizability and first-order hyperpolarizability, FMO and NBO analysis of 1-methyl-2-imidazolethiol. *Spectrochim. Acta Part A Mol. Biomol. Spectrosc.* **2014**, *118*, 999–1011. [[CrossRef](#)]
32. Schmid, F.X. Biological macromolecules: UV-visible spectrophotometry. In *eLS*; Wiley: Hoboken, NJ, USA, 2001.
33. Obi-Egbedi, N.; Obot, I.; El-Khaiary, M.; Umoren, S.; Ebenso, E. Computational simulation and statistical analysis on the relationship between corrosion inhibition efficiency and molecular structure of some phenanthroline derivatives on mild steel surface. *Int. J. Electrochem. Sci.* **2011**, *6*, e5675.
34. Tsuneda, T.; Song, J.-W.; Suzuki, S.; Hirao, K. On Koopmans' theorem in density functional theory. *J. Chem. Phys.* **2010**, *133*, 174101. [[CrossRef](#)]